

NUMERICAL INVESTIGATION OF IPE BEAMS STRENGTHENED AGAINST LATERAL-TORSIONAL BUCKLING

Marios Theofanous

Lecturer (ΠΔ 407/80)

Department of Civil Engineering, Aristotle University of Thessaloniki
Thessaloniki, Greece

e-mail: mariosgt@civil.auth.gr

Efthimios Koltsakis

Assistant Professor

Department of Civil Engineering, Aristotle University of Thessaloniki
Thessaloniki, Greece

e-mail: mkolts@civil.auth.gr

ABSTRACT

IPE sections are widely employed as beam members in a range of structural applications, owing to their structural efficiency when loaded about their major axis. However, their load carrying capacity decreases with increasing slenderness when no lateral restraint is provided, due to the occurrence of lateral torsional buckling (LTB). The present paper investigates the effectiveness of a novel means of enhancing the structural efficiency of IPE beams by welding side plates at the flange tips parallel to the section web at the beam ends, thereby providing an effective warping restraint. A comprehensive finite element study is conducted, which investigates the effect of the welded plates' geometry on both the critical buckling moment M_{cr} and the ultimate moment M_u of the considered beams over a wide range of IPE cross-sections and beam slendernesses. Moreover, a simplified analytical model is derived, which allows an accurate estimation of the critical buckling moment M_{cr} and thus of the non-dimensional slenderness $\bar{\lambda}_{LT}$ for a given cross-section and side plate geometry. Having established the non-dimensional slenderness, the ultimate capacity of the member can be determined following the provisions of EN 1993-1-1 [1].

1. INTRODUCTION

Numerous researchers have studied various means of enhancing the load carrying capacity of unrestrained beams with open cross-sections, with the focus lying on enhancing unrestrained I-beams. In cases of slender beams, the behaviour of which is governed by lateral torsional buckling, provision of bracing or additional restraint at the ends is an effective method of increasing the elastic critical buckling moment M_{cr} and hence the

ultimate capacity M_u , whilst more traditional strengthening techniques of increasing the in-plane capacity of a beam by welding plates on the flanges are less efficient.

Ojalvo and Chambers [2] proposed the use of box stiffeners at the beam ends, facilitated by welding channel sections with their axis perpendicular to the beam axis and their web parallel to the beam web. These stiffeners provide an effective restraint against warping and hence increase the elastic critical buckling moment M_{cr} . Plum and Svensson [3] further investigated the use of box stiffeners as warping restraints and derived a numerical method to determine the optimal placement of box stiffeners within a beam length for given load patterns. Szewczak et al. [4] examined the effectiveness of different configurations of stiffeners including side plates welded between the flange tips, which are in detail discussed in the present paper, whilst Murtha-Smith [5] focused on the behaviour of beams employing cross stiffeners. The influence of construction details of I beams, including end plates and notches, on their LTB response was studied by Lindner [6, 7]. More recently Liu and Gannon [8] conducted an experimental study on I-beams strengthened while under load with transverse stiffeners, side plates or flange plates.

The present paper investigates the effect of welded side plates (similar to the configuration studied in [4]) on the LTB response of IPE beams. The plates are welded between the flange tips at the beam ends in a similar fashion to the one reported in [8]; the details of the welding procedure and the required weld throat thickness are not considered herein. The plates are placed symmetrically at the beam ends with their height being equal to the distance between the flanges, whereas their aspect ratio and thickness is varied, and provide an effective warping restraint, thereby increasing both the elastic critical buckling moment M_{cr} and the ultimate moment M_u . The effect of the plate geometry is investigated over a wide range of IPE sections and beam lengths by means of geometrically and materially nonlinear finite element analysis, as described in the following Section.

2. NUMERICAL ANALYSIS

An extensive numerical study by means of the general purpose finite element analysis software ABAQUS [9] has been carried out to assess the effectiveness of the proposed strengthening technique for IPE beams susceptible to LTB. Twelve IPE sections (IPE 200 up to IPE 600) with four different lengths per cross-section (10h, 15h, 20h, 30h) have been modelled, thus encompassing a wide range of non-dimensional slendernesses $\bar{\lambda}_{LT}$ (0,73-2,13) commonly encountered in practice. All beams were simulated as simply supported under constant bending moment with fork supports (i.e. fixed torsion, free warping and rotation about the minor axis) at the ends. For each of the totally forty-eight beams considered, nine side plate geometries were investigated. In all cases the considered configuration consisted of four identical side plates, placed symmetrically with respect to the beam web and the beam midspan (two side plates per beam end, one on each side of the cross-section). The aspect ratio of the side plates c was set equal to either 0,5, 1 or 1,5, whilst the plate thickness t was a fixed fraction of the considered sections web thickness t_w (1/1,5/2).

The models were discretized with the reduced integration 4-noded doubly-curved general-purpose shell element S4R with finite membrane strains [9], which has performed well in similar studies [10]. Symmetry was exploited to reduce computational time and hence half the beam length was modelled, with suitable boundary conditions applied at midspan.

Kinematic coupling was employed to impose identical displacements between the beam flange tips and the attached side plates at their common nodes. The root radii of the IPE sections were modelled with the 3-noded Timoshenko beam element B33 [9], which was endowed with the torsional stiffness and the area of the root radii and was attached to the flange-web junction as a stringer. Failure to account for the root radii in numerical studies results in significant underpredictions, in terms of both stiffness (i.e. critical buckling moment) and ultimate capacity, due to the high torsional rigidity of the root radii. Lateral displacements of the end cross-sections were fixed along the web, thereby also preventing torsion, whereas the vertical displacement of the beam ends was restrained at mid-height of the web. The rotation of the stringers (simulating root radii) was also restrained at the end cross-section. The uniform bending moment was applied at the end cross-sections by imposing shell edge pressures along the flanges and the web, which were consistent with plastic stress distribution and the resultant of which was a unit moment. It was found however, that the models were relatively insensitive to the exact way the end moment was applied, with similar results being obtained even when the bending moment was applied as a pair of equal and opposite forces at the flange-web junctions.

The material model (elastic-perfectly plastic-strain-hardening) utilised by Taras and Greiner [11] to simulate steel grade S235 was adopted in the present study and was applied in the true stress-logarithmic plastic strain format. However in the vast majority of the performed simulations, failure occurred within the plastic plateau region and hence an elastic-perfectly plastic model would give identical results. Residual stresses were incorporated in the present study assuming the idealised distribution proposed in [11] and [12] and were applied as stress blocks having a constant value within each element; therefore a fine discretisation at cross-sectional level was employed, with sixteen elements along the flange width and the web height of each cross-section. The adopted material model and the applied residual stress distribution are depicted in Fig. 1. No residual stresses were imposed on the side plates, since for all considered cases both the side plates and the end parts of the beam to which the side plates were attached remained elastic at failure with stresses much lower than the yield stress; high inelastic stresses occurred at the mid-part of the beam. Moreover, as demonstrated in [8] where residual stress measurements of beams with welded side plates are reported, the welding residual stresses have a beneficial effect on the residuals stress distribution of the extreme parts of the beams, with tensile residual stresses occurring at the flange tips.

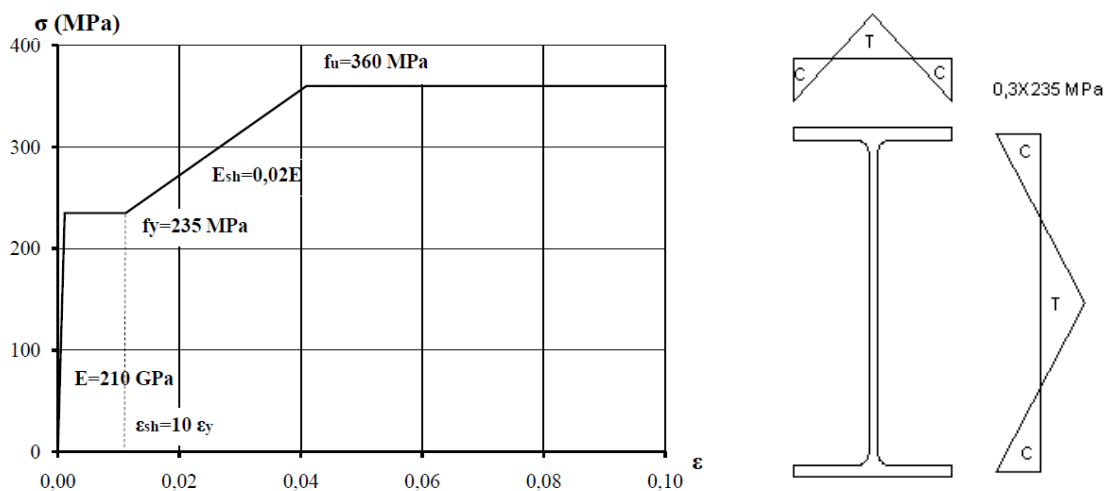


Fig. 1: Adopted material model and idealized residual stress distribution

A linear eigenvalue buckling analysis was initially conducted to extract the lowest buckling mode shape for each model, which in all cases corresponded to lateral torsional buckling. This was thereafter introduced as the geometric imperfection pattern in the subsequently performed geometrically and materially non-linear analyses. The amplitude of the geometric imperfection was set equal to $L/1000$ (L being the beam length) in accordance with similar studies [11, 12]. The non-linear analyses employed the modified Riks method [9], which enabled tracing the post-ultimate response of the modelled beams. For each beam cross-section and length considered, ten simulations were performed; the beam was initially simulated without any side plates in order to verify the validity of the generated numerical model and subsequently nine different side plate geometries (three aspect ratio variations and three thickness variations) were considered. The numerically obtained elastic critical buckling moment M_{cr} for the beams without side plates was on average 98% of the theoretical critical buckling moment M_{cr} with a coefficient of variation equal to 1%. The theoretical elastic critical buckling moment M_{cr} is given by Eq. (1) [13, 14] for a beam subjected to uniform bending moment, where k_z and k_w are effective length factors for the lateral buckling mode and the torsional buckling mode respectively, L is the actual beam length and the remaining symbols have their usual meaning.

$$M_{cr} = \frac{\pi}{k_z L} \sqrt{EI_z} \sqrt{GI_T + \frac{\pi^2 EI_w}{k_w L}} \quad (1)$$

Typical buckling mode shapes are depicted in Figs. 2 and 3 for a beam with and without side plates respectively. The ultimate moment obtained from the non-linear analyses for the beams without side plates is in good agreement with the predictions of EN 1993-1-1 [1], as shown in Table 1. The numerical results are presented in the following section.



Fig. 2: Lowest buckling mode shape for IPE 300 ($L=3000\text{mm}$)

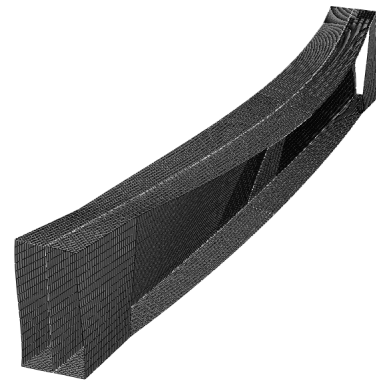


Fig. 3: Lowest buckling mode shape for IPE 300 ($L=3000\text{mm}$) with 300X300X7,1 side plates

$M_{b,Rd, EC3} / M_{b,Rd, ABAQUS}$	General case	Special case
MEAN	0,95	1,05
COV	0,04	0,02

Table 1: Numerical vs codified ultimate moment predictions

3. RESULTS AND DISCUSSION

Having demonstrated the validity of the generated FE models, the obtained numerical results are utilized to assess the effectiveness of the proposed strengthening method and to derive a simplified analytical method to predict the effect of welded side plates on the ultimate capacity of IPE beams subjected to uniform bending moment. More general loading cases (i.e. different bending moment diagrams and off-shear centre loading) can be treated by means of suitable modification factors available in the literature [13, 14]. In Fig. 4 the numerically obtained critical buckling moment M_{cr} of a beam with side plates with a thickness equal to the web thickness ($t=t_w$) is normalized by the respective moment of the non-strengthened beam $M_{cr,0}$ and plotted against the non-dimensional slenderness of the beam without side plates, whilst Fig. 5 depicts the effectiveness of the side plates in terms of the numerically obtained ultimate capacity.

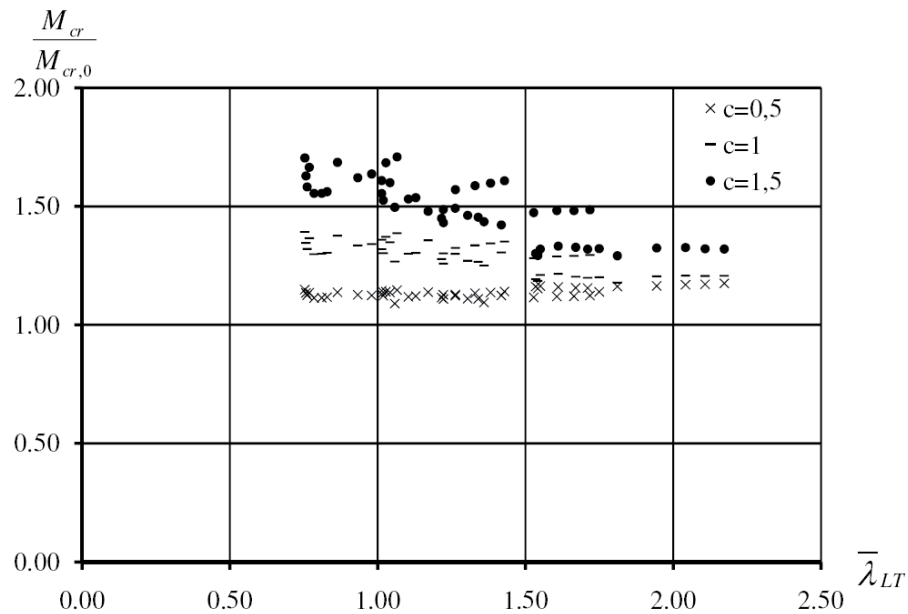


Fig.4: Normalized critical buckling moment for various plate aspect ratios c and $t=t_w$

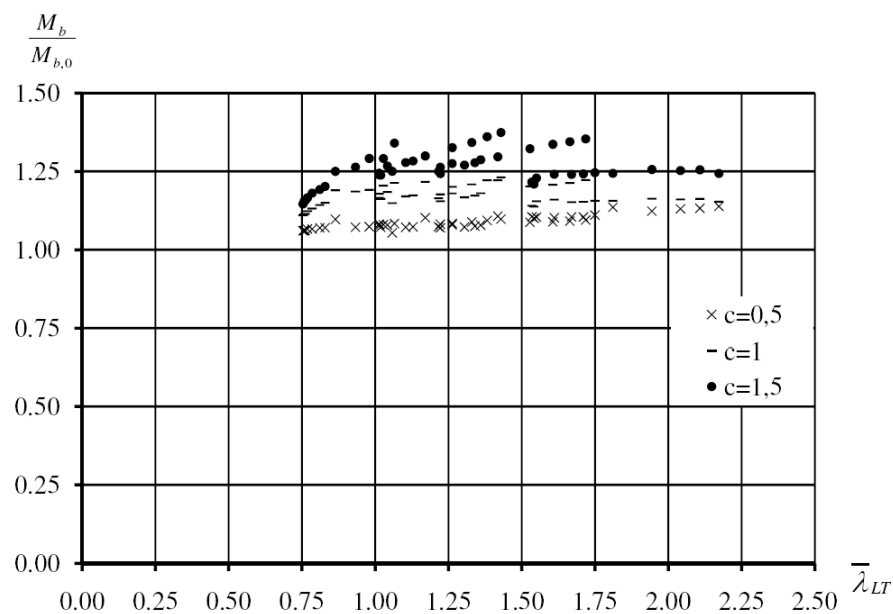


Fig.5: Normalized moment capacity for various plate aspect ratios c and $t=t_w$

In all performed simulations, the side plates remained elastic at failure with large inelastic strains occurring at the flange tips towards the central part of the beams. Hence it is reasonable to assume that the welded side plates provide an elastic warping restraint, the effect of which on the elastic critical buckling moment M_{cr} can be taken into account by means of the effective length factor k_w , corresponding to the torsional buckling mode, in Eq. (1). The effective length factor k_w can be estimated from Eq. (2), in accordance with similar studies [6, 7], where c_w is the restraint (i.e. warping spring stiffness) provided by the side plates to the end parts of the beam.

$$k_w = 1 - \frac{0.5}{1 + 2EI_w/c_w L} \quad (2)$$

In order to quantify the effect of the welded side plates, the beam is subdivided into three parts; the two outer parts of the beam containing the side plates with a length equal to $2ch_s$ (c being the aspect ratio of the side plates and h_s the height of the side plates) and the inner part with a length equal to $L-22ch_s$. The outer parts of the beam provide an additional torsional restraint to the inner part due to the side plates, which reduce the differential bending of the flanges by (i) enhancing the Saint-Venant torsional rigidity of the outer parts and (ii) connecting the top and the bottom flange, thus transferring warping stresses between the flanges, as shown in Fig. 6. The warping stresses of the flanges impose an equal and opposite rotation of the side plates, which is resisted by the flanges' flexural stiffness as schematically depicted in Fig. 7. The stiffness $c_{w,(i)}$ provided by mechanism (i) is given by Eq. (3), whilst the stiffness due to mechanism (ii) can be quantified on the basis of the simplified mechanical model depicted in Fig. 7.

$$c_{w,(i)} = \frac{ch_s^2 G}{3} (2t^3 + t_w^3) \quad (3)$$

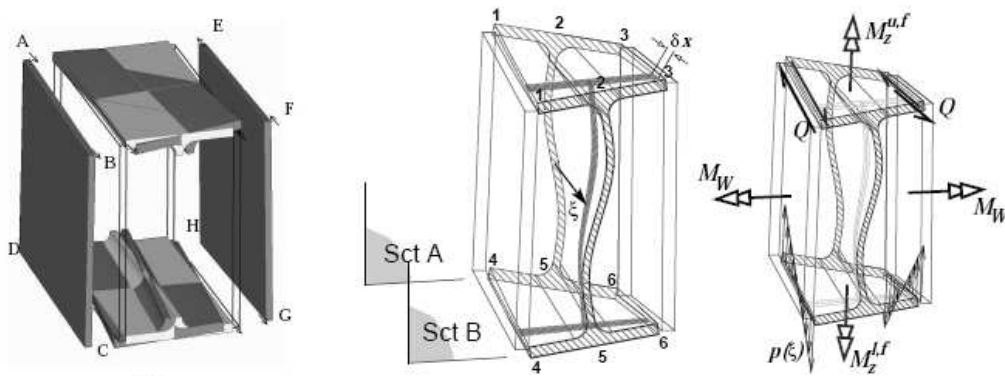


Fig. 6: Distortion and stresses transferred between the side plates and the flanges

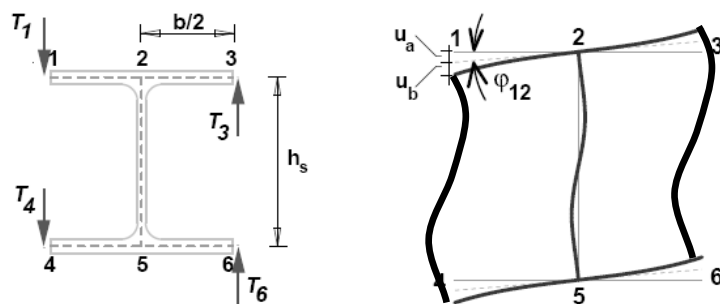


Fig. 7: Representation of a typical cross-section within an end part with beam elements

In Figs. 6 and 7 a beam end part and a typical cross-section within an end part is isolated and studied in order to determine the stiffness $c_{w,(ii)}$ contributed by mechanism (ii). Assuming that the side plates remain rigid within their plane, their rotation is resisted by the flanges as shown in Fig. 6, where the idealized as linear displacement profile imposed on the flange tips is also depicted. The warping stiffness $c_{w,(ii)}$ is given by Eq. (4), where h_s is the side plate flanges (distance between the flanges' centroids) and k_s is the flexural stiffness of the cross-section when subjected to the forces shown in Fig.7, which can be calculated from first principles, assuming beam behaviour.

$$c_{w,(ii)} = \frac{b \cdot (c \cdot h_s)^3 h_s}{3} \cdot k_s \quad (4)$$

Hence the total torsional stiffness provided by the end beam parts is the sum of $c_{w,(i)}$ and $c_{w,(ii)}$ and the effective length factor k_w is determined from Eq. (2). The critical buckling moment M_{cr} predicted following the proposed approach is on average 95% of the respective FE predictions with a coefficient of variation equal to 5%. Having obtained the critical buckling moment M_{cr} the load-carrying capacity of the beam can be determined, following the Eurocode 3 [1] approach. The ultimate moment $M_{b,Rd}$ is assumed to relate to the non-dimensional slenderness $\bar{\lambda}_{LT}$, which is readily obtained from the estimated M_{cr} . The accuracy of the simplified analytical method to account for the effect of the side plates on the ultimate capacity of the modeled beams is shown in Table 2 for both the general case and the special case set out in EN1993-1-1 [1], using the buckling curves codified for each case. Hence the proposed method is readily applicable within the framework of EN 1993-1-1 [1] and provides a rigorous estimation of the effect of welded side plates on both the critical buckling moment M_{cr} and the ultimate moment capacity $M_{b,Rd}$ of an I-beam.

$M_{b,Rd, EC3} / M_{b,Rd, ABAQUS}$	General case	Special case
MEAN	0,89	0,98
COV	0,05	0,04

Table 2: Numerical vs codified ultimate moment predictions for IPE beams employing side plates

4. CONCLUSIONS

A method of enhancing the LTB response of I-beams by welding side plates at the beam ends has been proposed in the present paper and its effectiveness has been investigated numerically for 12 cross-sections of the IPE series and four different lengths for every cross-section. Nine different side plate geometries have been considered and their effect on both stiffness and ultimate capacity has been determined. The generated FE models have been described in detail and were shown to be in good agreement with both the theoretical critical buckling moment M_{cr} and the ultimate capacity predictions codified in EN 1993-1-1 [1]. The effect of the side plates on the elastic critical buckling moment M_{cr} has been highlighted and quantified on the basis of a simplified analytical model, which has been shown to be in good agreement with the FE predictions. Finally the ultimate capacity $M_{b,Rd}$ is derived with reasonably good accuracy, following the provisions of EN 1993-1-1 [1]. The proposed strengthening technique can be applied in a variety of cases, is shown to be very efficient and is in principle applicable to all beams with employing an I-section.

6. REFERENCES

- [1] EN 1993-1-1 (2005) Eurocode 3. Design of Steel Structures: Part 1-1: General rules and rules for buildings. CEN.
- [2] Ojalvo, M. and Chambers, R.S. “Effect of warping restraints on I-beam buckling”. *Journal of the Structural Division, ASCE*, Vol. 103, No. 12, 1977, pp.2351-2360.
- [3] Plum, C.M. and Svensson, S.E. “Simple method to stabilize I-beams against lateral buckling”, *Journal of Structural Engineering*, Vol. 119, No. 10, 1993, pp. 2855-2870.
- [4] Szewczak, R.M., Smith, E.A. and De Wolf, J.T. “Beams with torsional stiffeners”, *Journal of Structural Engineering, ASCE*, Vol. 109, No. 7, 1983, pp. 1635-1647.
- [5] Murtha-Smith, E. “Cross stiffeners for beams in torsion”. *Journal of Structural Engineering*, Vol. 121, No. 7, 1995, pp. 1119-1124.
- [6] Lindner, J. “Influence of constructional details on the load carrying capacity of beams”, *Engineering Structures*, Vol. 18, No. 10, 1996, pp. 752-758.
- [7] Lindner, J. “Stability of structural members General Report”, *Journal of Constructional Steel Research*, Vol. 55, No. 1-3, 2000, pp. 29-44.
- [8] Liu, Y. and Gannon, L. “Experimental behavior and strength of steel beams strengthened while under load”, *Journal of Constructional Steel Research*, Vol. 65, No. 6, 2009, pp. 1346-1354.
- [9] ABAQUS/Standard user’s manual volumes I-III and ABAQUS CAE manual. Version 6.6. (Pawtucket, USA): Hibbitt, Karlsson & Sorensen, Inc; 2006.
- [10] Theofanous, M. and Gardner, L. “Experimental and numerical studies of lean duplex stainless steel beams”, *Journal of Constructional Steel Research*, Vol. 66, No. 6, 2010, pp. 816-825.
- [11] Taras, A. and Greiner, R. “New design curves for lateral-torsional buckling-Proposal based on a consistent derivation”, *Journal of Constructional Steel Research*, Vol. 66, No. 5, 2010, pp. 648-663.
- [12] Rebelo, C., Lopes, N., Simoes da Silva, L., Nethercot, D. and Vila Real, P.M.M. “Statistical evaluation of the lateral-torsional buckling resistance of steel I-beams,Part 1: Variability of the Eurocode 3 resistance model”, *Journal of Constructional Steel Research*, Vol. 65, No. 4, 2009, pp. 818-831.
- [13] Trahair, N.S., Bradford, M.A., Nethercot, D.A. and Gardner, L. “The behavior and design of steel structures to EC3”, Taylor & Francis, 2008.
- [14] Galambos, T.V. and Surovek A.E. “Structural stability of steel: concepts and applications for structural engineers”, John Wiley and Sons Inc, 2008.

ΑΡΙΘΜΗΤΙΚΗ ΔΙΕΡΕΥΝΗΣΗ ΜΕΘΟΔΟΥ ΕΝΙΣΧΥΣΗΣ ΔΟΚΩΝ ΙΡΕ ΕΝΑΝΤΙ ΣΤΡΕΠΤΟΚΑΜΠΤΙΚΟΥ ΛΥΓΙΣΜΟΥ

Μάριος Θεοφάνους
Λέκτορας (ΠΔ 407/80)
Τμήμα Πολιτικών Μηχανικών, Α.Π.Θ.
Θεσσαλονίκη, Ελλάδα
e-mail: mariosgt@civil.auth.gr

Ευθύμιος Κολτσάκης
Επίκουρος Καθηγητής
Τμήμα Πολιτικών Μηχανικών, Α.Π.Θ.
Θεσσαλονίκη, Ελλάδα
e-mail: mkolts@civil.auth.gr

ΠΕΡΙΛΗΨΗ

Στην παρούσα εργασία παρουσιάζεται μία μεθοδολογία ενίσχυσης δοκών διατομής διπλού Ταύ έναντι στρεπτοκαμπτικού λυγισμού μέσω της εισαγωγής “μέτρων παρακώλησης της καμπύλωσης” (ΜΠΚ), μέσω της εκατέρωθεν συγκόλλησης επιπέδων πλακών μεταξύ των άκρων των πελμάτων ενός διπλού Ταύ. Η διαφορική στροφή των πελμάτων του διπλού Ταύ οδηγεί τις πρόσθετες λεπίδες σε αντίρροπες στροφές περίξ του άξονα y της διατομής κατά EC3 (Σχ. 6). Στην κίνηση αυτή των προσθέτων πλακών αντιστέκεται ένας μηχανισμός “σίγμωσης” της διατομής (Σχ. 7) καθώς και ένας δεύτερος που συνιστά την κατά St Venant στρέψη των πρόσθετων λεπίδων συνάμα με την εγγύς σε αυτές περιοχή του κορμού του διπλού Ταύ. Οι δύο αυτοί κινηματικοί μηχανισμοί που ενεργοποιούνται από τα ΜΠΚ δίνουν μία δυσκαμψία έναντι καμπύλωσης c_w στο σημείο όπου εφαρμόζονται με συνακόλουθη απομείωση του συντελεστή k_w του στρεπτοκαμπτικού λυγισμού. Η προσπάθεια για την ποσοτικοποίηση της ευνοϊκής επίδρασης του παραπάνω μηχανισμού περιέλαβε δύο προσεγγίσεις. Αφενός την μελέτη της ενισχυμένης κατά τον ανωτέρω τρόπο δοκού με πεπερασμένα στοιχεία επιπέδου κελύφους με χρήση του λογισμικού ABAQUS και αφετέρου, με την μόρφωση αναλυτικών εκφράσεων για το ελατήριο διρροπής που προκύπτει ως συνέπεια της εισαγωγής των ΜΠΚ, σύμφωνα με τον κινηματικό μηχανισμό των Σχ. 6 και 7. Στο Σχ. 4 παρουσιάζεται η επίδραση των ΜΠΚ στην κρίσιμη ροπή στρέβλωσης ως συνάρτηση της λυγηρότητας στρέβλωσης $\bar{\lambda}_{LT}$ για τρία μήκη πλακών ΜΠΚ ($c = 50\%$, 100% και 150% του ύψους h_s της διατομής μεταξύ του κέντρου βάρους των πελμάτων) ενώ στο Σχ. 5 παρουσιάζεται η επίδραση των ΜΠΚ στην τελική αντοχή της δοκού κατά EC3. Στον Πίνακα 2 παρουσιάζεται η αποτίμηση των αποτελεσμάτων της προτεινόμενης αναλυτικής προσέγγισης σε σχέση με τα λαμβανόμενα από την ανάλυση FEM. Ως συμπέρασμα των αποτελεσμάτων που προέκυψαν διαπιστώθηκε η αποτελεσματικότητα της προτεινόμενης μεθόδου ενίσχυσης των δοκών ΙΡΕ έναντι στρεπτοκαμπτικού λυγισμού και οι δυνατότητες χρήσης της στα πλαίσια των ελέγχων του EC3.